The effect of swift heavy ion irradiation on perpendicular magnetic anisotropy in Fe-Tb multilayers

1998 J. Phys.: Condens. Matter 10 9669

(http://iopscience.iop.org/0953-8984/10/43/009)

J. Phys.: Condens. Matter **10** (1998) 9669–9680. Printed in the UK PII: S0953-8984(98)91455-2

The effect of swift heavy ion irradiation on perpendicular magnetic anisotropy in Fe–Tb multilayers

Ajay Gupta†, Amitesh Paul†, Ratnesh Gupta‡, D K Avasthi§ and G Principi‖

† Inter-University Consortium for DAE Facilities, Khandwa Road, Indore 452017, India
‡ Institute of Instrumentation, DA University, Khandwa Road, Indore 452017, India
§ Nuclear Science Centre, Aruna Asaf Ali Marg, PO Box 10502, New Delhi 110067, India
‖ Dipartimento di Ingegneria Meccanica, Universita di Padova, via Marzolo 9, 35131 Padova, Italy

Received 9 February 1998, in final form 10 June 1998

Abstract. The effect of swift heavy ion irradiation of Fe–Tb multilayers has been studied using x-ray reflectivity and conversion electron Mössbauer spectroscopy measurements. The energy deposited in the multilayer in the form of electronic excitations results in significant modification of the interfaces. During 80 MeV Si ion irradiation the interfacial roughness is found to increase linearly with irradiation dose. Mössbauer measurements provide evidence of segregation of Fe and Tb atoms in the intermixed region, which may be the cause of the observed increase in the interfacial roughness. The as-deposited multilayer exhibits a large perpendicular magnetic anisotropy, which shows a monotonic decrease with irradiation dose. The observed decrease in perpendicular magnetic anisotropy is a combined effect of the stress relaxation in the bulk of layers and an increase in the interfacial roughness. 150 MeV Ag ion irradiation causes additional intermixing at the interface, accompanied by a large reduction in perpendicular magnetic anisotropy.

1. Introduction

The existence of a uniaxial perpendicular magnetic anisotropy (PMA) in transition metal–rare earth (TM–RE) multilayers such as Fe/Tb, Dy/Fe etc make them important as potential magneto-optical recording media. PMA shows a strong variation with the thickness of RE and TM layers, as well as with the state of the RE/TM and TM/RE interfaces [1–5]. The origin of magnetic anisotropy in these systems is not yet fully understood, although it is generally agreed that the dominant contribution to PMA originates from the single ion anisotropy of the rare earth ions coupled with the anisotropic distribution of TM–RE bonds at the interfaces [1, 2, 7]. Fe–Tb multilayers shows a higher value of PMA as compared to the other TM–RE systems, and therefore have been studied extensively with regard to their structural and magnetic properties. In Fe–Tb multilayers, with increasing layer thickness the crystallographic structure of the Fe layer changes from an amorphous to crystalline bcc structure around a critical thickness d_c of 2.0–2.4 nm [3, 4]. For both the amorphous and the crystalline structure of the Fe layer, the multilayer shows PMA which sensitively depends upon the state of the interface between Fe and Tb layers. Detailed depth selective conversion electron Mössbauer spectroscopy shows that Fe/Tb and Tb/Fe interfaces are not equivalent and that the PMA mainly originates from the Tb-on-Fe interface [6].

0953-8984/98/439669+12$19.50

The magnitude of PMA also depends upon the thickness of the intermixed layer between the Fe and Tb layers. The effect of annealing on a set of Fe–Tb multilayers in which the structure of Fe layers was amorphous showed that the PMA varies inversely with the thickness of the intermixed layer [8]; annealing at 100 °C causes a demixing at the interface, which results in a decrease in the thickness of the interfacial region and an increase in PMA, while annealing at higher temperatures causes the thickness of the intermixed region to increase, accompanied by a decrease in PMA. In Fe–Tb multilayers having crystalline bcc Fe layers, increase in the thickness of the intermixed layer due to variations in the substrate temperature has been found to increase the PMA [9]. On the other hand, both demixing and mixing at the interface induced by heavy ion irradiation causes PMA to decrease [10, 11].

The irradiation effects of swift heavy ions are quite complex and depend upon the electronic energy loss $(\mathrm{d}E/\mathrm{d}X)_e$ as well as the thicknesses of the Fe and Tb layers. Using a variety of ion species and energies Richomme *et al* [10, 11] have covered a range of $(\mathrm{d}E/\mathrm{d}X)_e$ from 15 to 56 keV nm^{-1} in the study of multilayers with Fe layer thicknesses both below and above the critical thickness d_c. Depending upon the values of $(\mathrm{d}E/\mathrm{d}X)_e$ three distinct types of effect of ion irradiation have been observed. (i) For values of $(\mathrm{d}E/\mathrm{d}X)_e$ below 17 keV nm^{-1} irradiation results in segregation of Fe and Tb atoms in the interfacial region. The segregation effect is pronounced in multilayers with Fe thickness close to the critical thickness of 2.2 nm. (ii) For the case of 30 keV nm$^{-1} \leqslant (\mathrm{d}E/\mathrm{d}X)_e \leqslant 52$ keV nm^{-1}, with increasing irradiation dose initially a small demixing effect is observed, while for higher doses strong intermixing takes place and finally for sufficiently high doses a homogeneous amorphous Fe–Tb alloy is obtained. (iii) For $(\mathrm{d}E/\mathrm{d}X)_e$ values above 52 keV nm^{-1}, instead of intermixing the pronounced effect is the amorphization of the bulk of the Fe layers.

The PMA has been found to decrease with irradiation dose in the case of demixing as well as mixing. It has been argued that although the sharpening of interfaces due to demixing should have resulted in an increase in PMA, an increase in the thickness of the α-Fe layer causes the shape anisotropy to increase and thus the net effect of the two is to decrease the PMA. It may be pointed out here that the observed variation in PMA with irradiation in the above mentioned works [10, 11] cannot be understood only in terms of a change in the thickness of the intermixed layer. For example, the effect of the increase in α-Fe thickness from 53 to 57% of the total iron content due to Kr irradiation causes the angle ϕ between the average spin direction and the film normal to increase from 68 to 75°. A similar change in the thickness of α-Fe produced by either Xe or Pb irradiation does not cause any change in the angle ϕ within experimental error. Thus, in order to understand the observed variation in PMA, effects of irradiation other than demixing or mixing should also be considered.

In the present work we have studied the effect of 80 MeV Si ion irradiation of Fe–Tb multilayers. The $(\mathrm{d}E/\mathrm{d}X)_e$ value in the present case is far below the range studied by Richomme *et al* [10, 11]: for this value of $(\mathrm{d}E/\mathrm{d}X)_e$ some additional disorder in the system is expected to occur without any additional intermixing at the interfaces. The aim of the present work is to study the effect of such interfacial modifications on the PMA. For comparison, the effect of 150 MeV Ag ion irradiation, where one expects some interfacial mixing to occur, has also been studied.

2. Experimental details

The multilayer consisted of 20 bilayers of composition 3.0 nm Fe/2.0 nm Tb, deposited on a Si substrate with 100.0 nm of thermally grown amorphous SiO_2. An extra layer of Fe

was deposited on top of the last Tb layer. Deposition was performed in a vacuum better than 3×10^{-7} Pa.

Multilayers were irradiated with 80 MeV Si ions using the 15UD Pelletron facility of the Nuclear Science Centre, New Delhi. The vacuum inside the irradiation chamber was of the order of 10^{-5} Pa. The incident ion flux was 18.6×10^9 ions s^{-1} cm^{-2}. Two different samples were irradiated to total fluences of 10^{14} and 10^{15} ions cm^{-2} respectively. The projected range of 80 MeV ions in the multilayer as calculated using TRIM95 code is about 15 μm, which is greater than the total thickness of the multilayer. Thus the bombarding ions pass through the entire Fe–Tb stack. The calculated average electronic and nuclear stopping powers within the multilayer are respectively 6.0 keV nm^{-1} and 5.8 eV nm^{-1}. Therefore, the damage created in the multilayer is entirely due to electronic excitations.

The specimen irradiated with 10^{15} ions cm^{-2} of 80 MeV Si ions was subsequently given another irradiation with 150 MeV Ag ions to a fluence of 10^{13} ions cm^{-2}. The average electronic stopping powers for 150 MeV Ag ions in the multilayer is 27.1 keV nm^{-1}, which is close to threshold for intermixing [11, 12]. The specimens were characterized before and after irradiation using x-ray reflectivity and Mössbauer measurements.

For x-ray reflectivity a powder x-ray diffractometer model D5000 from Siemens with Cu Kα radiation was used. In order to limit divergence of the x-ray beam, a 50 μm slit was introduced in the path of the incident x-rays and a knife edge was kept touching the surface of the specimen. The micrometre size gap between the film surface and the knife edge acts as a narrow slit. The reflectivity pattern was measured in the 2θ range of 0.2–4.0°. The corresponding momentum transfer vector $q = (4\pi \sin\theta)/\lambda$ varies in the range of 0.14–2.84 nm^{-1}. For such small values of momentum transfer vector, the response of the medium to the x-rays can be characterized by a refractive index.

$$n = 1 - \delta - \mathrm{i}\beta$$

where, in the x-ray region, both δ and β are positive and of the order of 10^{-5}–10^{-7}. The dispersive and absorption correction terms δ and β are given by [13, 14]

$$\delta = \frac{Ne^2\lambda^2(Z + f')}{2\pi mc^2} \qquad \beta = \frac{Ne^2 f''}{2mc^2}$$

where N is the number density of atoms and f' and f'' are respectively the resonance and absorption corrections to the atomic scattering factor arising from anomalous dispersion. Below a critical angle $\theta_c = (2\delta)^{1/2}$, x-rays are totally reflected from the surface. For an angle of incidence $\theta > \theta_c$, the Fresnel coefficient for reflection from the interface between jth and $(j+1)$th layers is given by

$$F_{j,j+1} = \frac{E_j^R}{E_j} = \frac{(g_j - g_{j+1})}{(g_j + g_{j+1})}$$

with $g_j = (n_j^2 - \cos^2\theta)$. E_j and E_j^R are amplitudes of the electric vector of the incident waves and waves reflected from the interface respectively and n_j is the refractive index of the jth layer. Using the boundary condition that the tangential components of the electric vector be continuous at the interface, a recursion relation for the reflection coefficient is obtained [15].

$$R_{j,j+1} = a_j^4 \frac{R_{j+1,j+2} + F_{j,j+1}}{R_{j+1,j+2}F_{j,j+1} + 1}$$

where $a_j = \exp(-\mathrm{i}\pi g_j t_j/\lambda)$ is the amplitude factor for half the perpendicular distance t_j, the thickness of the jth layer. The computation starts at the substrate and works recursively back to the first surface where the value of R_{01} is arrived at. The resulting reflectivity is

$I/I_0 = (R_{12})^2$. The effect of the interfacial roughness σ is incorporated by multiplying the Fresnel coefficient $F_{j,j+1}$ by a factor [13, 16]

$$b_{j,j+1} = \exp(-2k_j k_{j+1}\sigma_{j+1}^2)$$

where σ is the rms roughness and the scattering vector

$$k_j = 2\pi \frac{g_j}{\lambda}.$$

The observed reflectivity pattern contains information about the surface and interface roughnesses, thicknesses of the individual layers, interdiffusion etc [13]. A computer program based on the above algorithm has been developed in order to generate the reflectivity pattern of the multilayers. The theoretically generated reflectivity pattern was compared with the experimental data in order to extract the relevant information about the specimens.

^{57}Fe conversion electron Mössbauer spectra were recorded at room temperature using a flowing gas (95% He, 5% CH_4) proportional counter and a 25 mCi ^{57}Co source in an Rh matrix. The spectral profiles were analysed by means of the NORMOS code developed by Brand [17]. Each Mössbauer spectrum was fitted with two distributions—one corresponding to the relatively sharp sextet due to bulk α-Fe in a layer and the other corresponding to iron atoms in the interface regions. While for the first distribution (the component of α-Fe) a Gaussian shape was assumed, for the second distribution the histogram method was used. Since both hyperfine field and isomer shift at a given iron site depend upon the number of Tb near neighbours and their distances, a correlation between B_{hf} and isomer shift is expected in the interfacial region; therefore the second distribution is fitted by taking a linear correlation between hyperfine field and isomer shift. The relative intensities X of the second and third lines for both the distributions were constrained to be equal and taken as a fitting parameter.

3. Results

3.1. X-ray reflectivity measurements

Figure 1 gives the x-ray reflectivity pattern of the virgin as well as the irradiated specimens. The first and second order Bragg peaks due to multilayer periodicity are distinctly visible. The critical angle for the total reflection is obtained as $\theta_c = 0.316^\circ$ which is lower than that for either Fe or Tb. This suggests that the surface of the film is contaminated with oxygen or some other contaminant causing the electron density at the surface to decrease. For the theoretical fit to the experimental data, the multilayer was considered to consist of alternating layers of Fe and Tb with an intermixed layer of composition $Fe_{0.5}Tb_{0.5}$ at each interface. A thin layer of oxide was also assumed at the top. The refractive indices of Fe and Tb layers were taken to be those of bulk materials, while that of the FeTb intermixed layer was taken to be the average of those for Fe and Tb. To fit the experimental data the following quantities were taken as parameters: (i) thickness of the top oxide layer, (ii) the intermixed layer at the interfaces and (iii) roughnesses of the top surface and the subsequent interfaces. It may be noted that each of the above parameters affects a different aspect of the reflectivity curve. Therefore, although a number of parameters are used to fit the experimental data, the values of individual parameters obtained from the best fit are quite reliable. In order to make this point clear, figure 2 shows a simulated reflectivity pattern of an Fe–Tb multilayer with different combinations of interface roughness, interdiffusion and top oxide layer. From figure 2, one may note that (i) the roughness affects the overall

decay rate of the envelope of the reflectivity curve while (ii) the intermixing at the interface affects height of the Bragg peaks, specially that of the second one. (iii) The effect of the top oxide layer is to produce a periodic modulation of the reflectivity curve and the period depends on the thickness of the oxide layer [18].

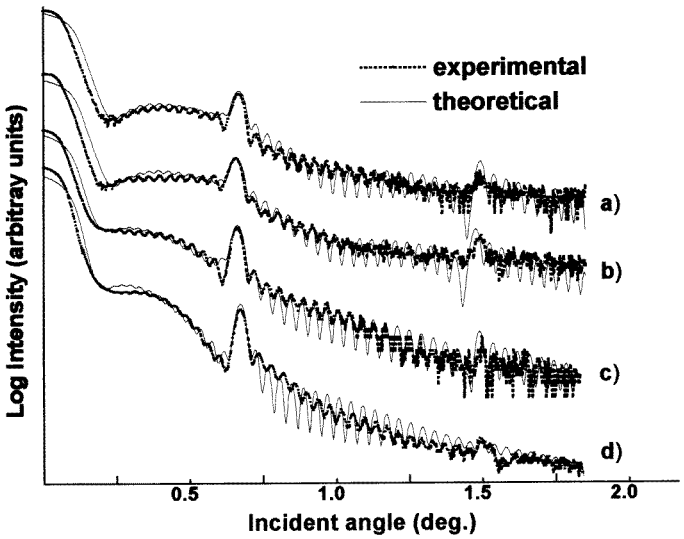

Figure 1. X-ray reflectivity pattern of Fe(3 nm)–Tb(2 nm) multilayers: (a) as-deposited film; (b), (c) film after 80 MeV Si ion irradiation with a dose of (b) 10^{14} ion cm^{-2} and (c) 10^{15} ion cm^{-2}. Curve (d) corresponds to a further irradiation of specimen (c) by 150 MeV Ag ions to a dose of 10^{13} ions cm^{-2}. The continuous curves represent the best theoretical fit to the experimental data.

The theoretical curve which best fits the experimental data is shown as a continuous curve in figure 1. The corresponding fitted parameters are given in table 1. One may note that even in the as-deposited film the interface between Fe and Tb is not very sharp. About 1.0 nm of interdiffused layer exists at each interface. The roughness of interfaces is about 0.2 nm, while that of the top surface is 1.0 nm. The theoretical fit to the data shows that the main effect of the irradiation up to the highest dose of Si is to increase the interfacial roughness to a value of 0.65 nm. No significant increase in the thickness of the intermixed layer is observed. Ag ion irradiation causes both the interfacial roughness and the intermixed region to increase.

3.2. Mössbauer measurements

Figure 3 shows the room temperature CEMS spectra before and after irradiation. The spectra have been analysed assuming a superposition of two hyperfine field distributions in section 2. The results of the fitting are summarized in table 2.

The magnetic texture of the sample is revealed by the intensity X of the middle peaks relative to the inner ones of the Mössbauer spectrum. Theoretically, the intensities of the peaks are in the ratio $3{:}X{:}1{:}1{:}X{:}3$, with

$$X = \frac{4\sin^2\phi}{(1+\cos^2\phi)} \tag{1}$$

Table 1. Parameters and refinement results of Fe(3 nm)–Tb(2 nm) multilayers on Si substrate before and after irradiations. For individual layers, t is the layer thickness, δ and β are respectively the dispersive and absorption corrections to the refractive index and σ is the roughness of the interface with the adjacent layer on top of it. Values of the fitted parameters are given up to the last significant digit.

Ion species	Irradiation dose (ions cm^{-2})	Layer	t (nm)	δ ($\times 10^{-6}$)	β ($\times 10^{-6}$)	σ (nm)
Si	0.0	oxide	5.3	10.5	2.70	1.00
		FeTb	0.5	20.6	3.00	0.20
		Tb	1.05	18.8	3.08	0.20
		FeTb	1.0	20.6	3.00	0.20
		Fe	2.2	22.5	2.90	0.20
		19× FeTb	1.0	20.6	3.00	0.20
		19× Tb	1.05	18.8	3.08	0.20
		19× FeTb	1.0	20.6	3.00	0.20
		19× Fe	2.2	22.5	2.90	0.20
		SiO_2	100	8.02	0.106	0.20
		Si	∞	7.59	0.173	0.20
Si	1×10^{14}	oxide	5.3	10.5	2.70	1.00
		FeTb	0.5	20.6	3.00	0.25
		Tb	1.05	18.8	3.08	0.25
		FeTb	1.0	20.6	3.00	0.25
		Fe	2.25	22.5	2.90	0.25
		19× FeTb	1.0	20.6	3.00	0.25
		19× Tb	1.05	18.8	3.08	0.25
		19× FeTb	1.0	20.6	3.00	0.25
		19× Fe	2.2	22.5	2.90	0.25
		SiO_2	100	8.02	0.106	0.25
		Si	∞	7.59	0.173	0.20
Si	1×10^{15}	oxide	6.0	10.5	2.70	1.50
		FeTb	0.5	20.6	3.00	0.65
		Tb	1.05	18.8	3.08	0.65
		FeTb	1.0	20.6	3.00	0.65
		Fe	2.2	22.5	2.90	0.65
		19× FeTb	1.0	20.6	3.00	0.65
		19× Tb	1.05	18.8	3.08	0.65
		19× FeTb	1.0	20.6	3.00	0.65
		19× Fe	2.2	22.5	2.90	0.65
		SiO_2	100	8.02	0.106	0.40
		Si	∞	7.59	0.173	0.20
Si	1×10^{15}	oxide	6.4	10.5	2.70	1.50
+		FeTb	1.2	20.6	3.00	1.00
Ag	1×10^{13}	Tb	0.5	18.8	3.08	1.00
		FeTb	1.2	20.6	3.00	1.00
		Fe	2.0	22.5	2.90	1.00
		19× FeTb	1.2	20.6	3.00	1.00
		19× Tb	0.85	18.8	3.08	1.00
		19× FeTb	1.2	20.6	3.00	1.00
		19× Fe	2.0	22.5	2.90	1.00
		SiO_2	100	8.02	0.106	0.40
		Si	∞	7.59	0.173	0.20

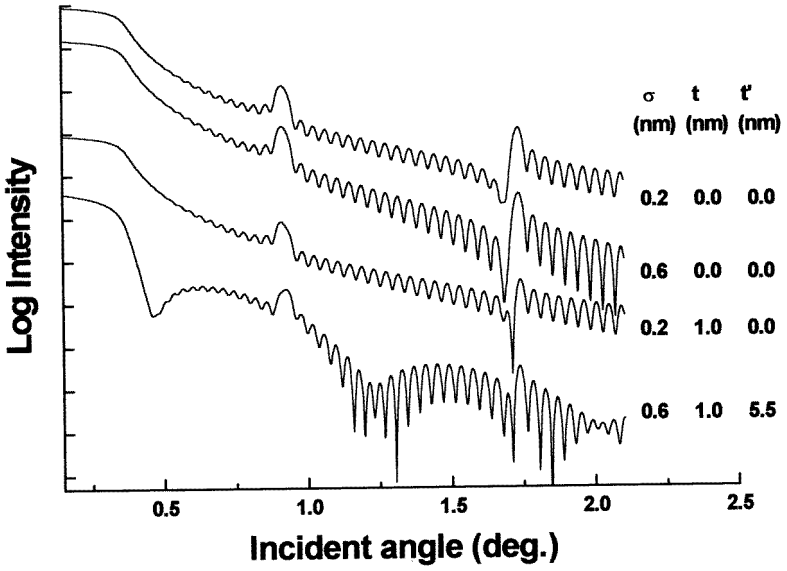

Figure 2. Simulated reflectivity patterns for Fe(3 nm)–Tb(2 nm) multilayer with different values of the surface and interface roughnesses σ, thickness t of interdiffused layer and the thickness t' of the top oxide layer. It may be noted that each of these parameters affects a different aspect of the reflectivity curve.

Table 2. Results of computer fitting of CEMS spectra of the studied Fe(3 nm)–Tb(2 nm) multilayers on Si substrate before and after irradiations. The uncertainties of the values as obtained from the least squares fitting routine are also reported. The error in ϕ, the angle between the average spin direction and the film normal is calculated using equation (1) and the error in X obtained from the fitting routine. $\langle B_{hf}(\mathrm{T})\rangle$ and $\Delta B_{hf}(\mathrm{T})$ are the average value and the standard deviation of the field distribution corresponding to the α-Fe component. A_α represents the percentage area of the total spectrum in the α-Fe subspectra. A_{25-35}/A_{0-35} is the percentage of the field area under the broad component which lies between the B_{hf} values $25\ \mathrm{T} \leqslant B_{hf} \leqslant 35\ \mathrm{T}$.

		Parameters of the α-Fe component				
Ion species	Irradiation doses (ions cm^{-2})	$\langle B_{hf}(\mathrm{T})\rangle$	$\Delta B_{hf}(\mathrm{T})$	A_α relative area (%)	ϕ (°)	$\frac{A_{25-35}}{A_{0-35}}$ (%)
Si	0.0	33.34 ± 0.02	0.69 ± 0.02	54 ± 1	33.6 ± 1.0	72
Si	1×10^{14}	33.28 ± 0.01	0.69 ± 0.02	55 ± 1	36.1 ± 1.0	73
Si	1×10^{15}	33.17 ± 0.02	0.70 ± 0.02	54 ± 1	39.9 ± 1.0	74
Si + Ag	1×10^{15} / 1×10^{13}	35.15 ± 0.03	0.61 ± 0.05	47 ± 1	62.2 ± 1.2	42

where ϕ is the angle between the γ-ray direction, which is normal to the film plane, and the average direction of the magnetic moments of the iron atoms. An increase in PMA results in a decrease in the value of ϕ. The value of ϕ as calculated using the fitted parameters is also shown in table 2.

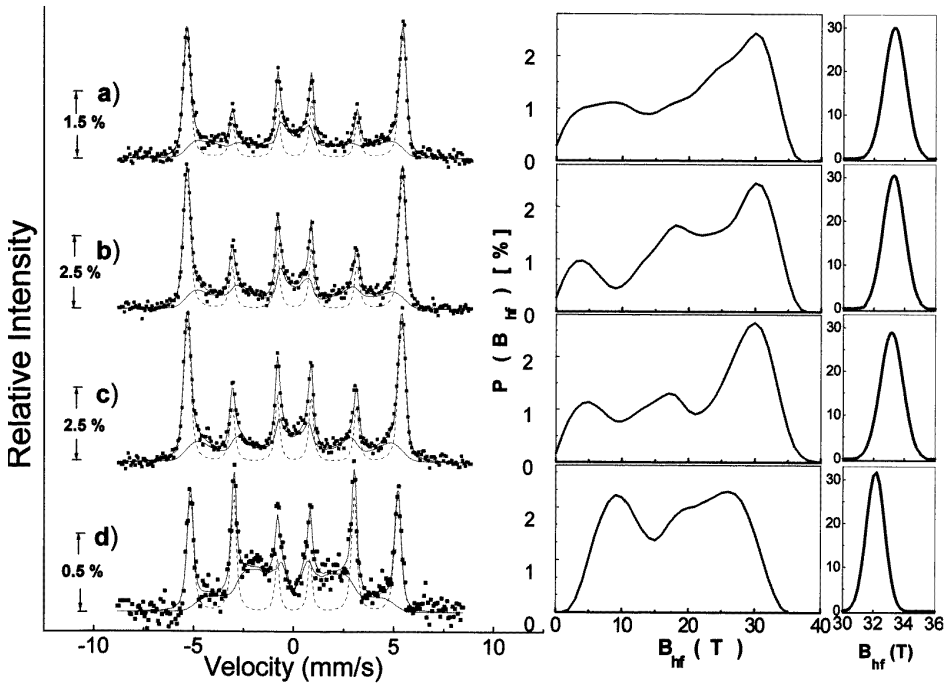

Figure 3. CEMS spectra of Fe(3 nm)–Tb(2 nm) multilayers: (a) as-deposited film; (b), (c) film after 80 MeV Si ion irradiation with a dose of (b) 10^{14} ions cm^{-2} and (c) 10^{15} ions cm^{-2}. Curve (d) corresponds to a further irradiation of specimen (c) by 150 MeV Ag ions to a dose of 10^{13} ions cm^{-2}. The continuous curves represent the best fit to the experimental data obtained by taking two independent hyperfine field distributions corresponding to the sharp sextet representing bulk α-Fe and the remaining broad component representing the interfacial region. The evaluated hyperfine field distributions are also shown. It may be noted that the vertical scales of the two distributions are different.

A qualitative estimate of thickness of the intermixed layer as obtained from the Mössbauer measurements agrees reasonably well with that obtained from the x-ray reflectivity data. From the fitting of the Mössbauer data one finds that the area under the broad hyperfine component which has contributions from Fe atoms at the interface as well as in the intermixed layer is about 4%. If one neglects the difference in the recoilless fractions of the iron atoms in the bulk α-Fe layer and in the interfacial regions, one can take 45% of the Fe atoms as residing in the interfacial region. For perfectly sharp interfaces two monolayers of each of Fe layer will be interfaced with Tb atoms. This will constitute about 10% of the total atoms in a layer. Therefore $45 - 10 = 35\%$ of Fe atoms exist in the intermixed layers. On the other hand, from the fitting of the x-ray reflectivity data, the thickness of the intermixed layer is about 1.0 nm. Taking the composition of the intermixed layer as $Fe_{0.5}Tb_{0.5}$, this thickness corresponds to about 30% of Fe atoms in the intermixed region.

Irradiation to the highest dose does not cause any change in the area under the broad hyperfine component, indicating that irradiation of Si does not cause any further intermixing at the interfaces. From table 2 it may be noted that after the highest dose of irradiation the average hyperfine field of the unmixed α-Fe layer decreases from 33.34 to 33.17 T. This

change in the hyperfine field of α-Fe is indicative of the creation of some disorder in the bulk of the Fe layer. The most significant effect of irradiation is observed on the PMA. The angle ϕ increases from 33.6° for the virgin sample to 39.9° for the sample with the highest irradiation dose, indicating a decrease in PMA upon irradiation.

Irradiation with 150 MeV Ag ions results in a decrease in the unmixed α-Fe region by ∼7% accompanied by a large decrease in PMA.

4. Discussion

Both x-ray reflectivity and Mössbauer measurements show that irradiation with Si ions does not induce any additional intermixing at the interface. However the x-ray reflectivity measurements show a distinct increase in the interface roughness upon irradiation. Figure 4 shows that the roughness increases almost linearly with irradiation dose. From the same figure it may be noted that, in contrast to the interface roughness, PMA does not show a linear variation with irradiation dose.

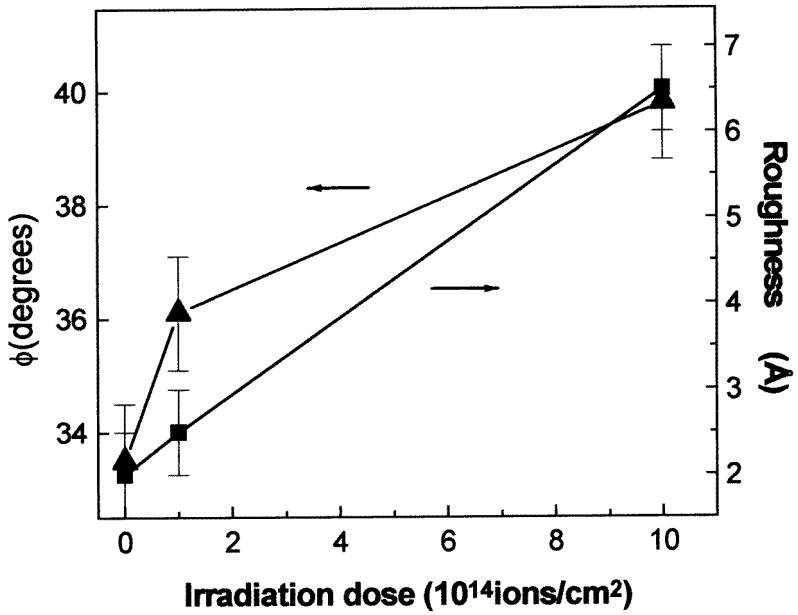

Figure 4. The variation of the interfacial roughness and the angle ϕ with the dose of irradiation with 80 MeV Si ions.

Several studies have indicated that the energy deposited in the target due to electronic excitation $(\mathrm{d}E/\mathrm{d}X)_e$ during the passage of swift heavy ions can induce structural modifications in metallic systems [19–22]. The observed effects include creation of point defects [19], phase transformation [20], latent track formation [21] and intermixing at the interface [22]. However, in metals the threshold value of $(\mathrm{d}E/\mathrm{d}X)_e$ above which significant damage can occur is much higher than that in insulators. In the case of 80 MeV Si ions $(\mathrm{d}E/\mathrm{d}X)_e$ as calculated using the TRIM95 code is 6.9 and 4.7 keV nm^{-1} in Fe and Tb layers respectively. These values are much smaller than the reported threshold values of 25 keV nm^{-1} for latent track formation or intermixing in Fe [12]. Thus, we do not expect any intermixing to occur under the irradiation conditions used in the present experiment.

However the creation of point defects in metals or their annihilation may occur at $(\mathrm{d}E/\mathrm{d}X)_e$ values much smaller than the threshold for latent track formation. Thus, the values of $(\mathrm{d}E/\mathrm{d}X)_e$ achieved in the present case may be sufficient to produce isolated point defects and short range movement of atoms. Such processes would be responsible for the creation of disorder in the bulk of Fe and Tb layers, causing the observed changes in the hyperfine field parameters of α-Fe layers, and may also cause the surface roughness to increase.

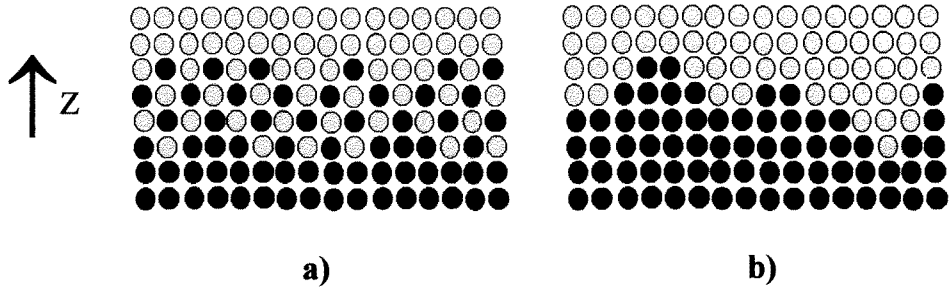

Figure 5. A schematic view of the distribution of atoms of two species at the interface (a) in the presence of finite interdiffusion and (b) after a partial segregation of Fe and Tb atoms.

Perusal of the distribution of the broad hyperfine component (figure 3) shows that with increasing dose of irradiation the low field tail of the distribution decreases while the probability around 30 T increases in magnitude. However the total area under the distribution curve remains unchanged. Thus, although irradiation does not cause any change in the thickness of the intermixed layer, the observed changes in the shape of hyperfine field distribution provide evidence for the incipient demixing between Fe and Tb layers; a segregation of Fe and Tb atoms would cause an increase in the population of Fe atoms with smaller number of Tb near neighbours at the expense of the population of Fe atoms with larger number of Tb near neighbours, thus resulting in a shift of the probability from the lower hyperfine field region to the higher hyperfine field region. In order to quantify the demixing effect the fractional area under the broad hyperfine field component was divided into two parts covering the hyperfine field ranges from 0 to 25 T and 25 to 35 T. As seen from table 2, the area under the hyperfine field range 25–35 T shows a systematic increase with irradiation dose. This quantity may be taken as a measure of the degree of demixing in the interface layer. As shown schematically in figure 5, such segregation would also cause an increase in the interfacial roughness: assuming a perfectly flat and sharp interface in the beginning, an intermixing at the interface which is uniform in the x–y plane would cause a gradient of the iron concentration along the z direction (figure 5(a)). However, a surface of constant concentration will still remain flat. On the other hand, segregation of Fe and Tb atoms would modify the topology of the surface of constant concentration and, thus, would cause the interface roughness to increase (figure 5(b)).

The electronic energy loss $(\mathrm{d}E/\mathrm{d}X)_e$ associated with 150 MeV Ag ions is just above the threshold for intermixing as observed by Teillet *et al* [11], and thus, as expected, causes an additional intermixing at the interfaces.

The magnetic anisotropy of the magnetic layers with thickness t can be phenomenologically written as [23, 24]

$$K = K_v + 2K_s/t$$

the volume term, K_v, contains contributions from shape, magnetocrystalline and

magnetoelastic anisotropies, while K_s is the interface contribution. Shape anisotropy would always try to keep atomic spins in the film plane in order to minimize the magnetostatic energy. The magnitude of the shape anisotropy will also depend upon the magnetic moment per iron atom and thus upon the structure of the Fe layer. In the case where the structure of the Fe layer is amorphous, the magnetic moment per iron atom is small and hence the shape anisotropy will be weak. The magnetocrystalline anisotropy depends upon the crystal structure of the layers which for hcp structure (e.g. Co) may be quite high; however for Fe layers with bcc this anisotropy is small. Magnetoelastic anisotropy has its origin in the internal stresses present in the individual layers. The stresses may arise by differences in thermal expansions between film and substrate or between the layers. Structural defects may also give rise to internal stresses. The interface anisotropy K_s in RE–TM multilayers has its origin in single ion anisotropy coupled with anisotropic distribution of RE–TM pairs [1]. In the present case the only observed change at the interface is an increase in the interfacial roughness without any change in the thickness of the intermixed layer. Therefore the observed decrease in PMA with irradiation dose suggests that an increase in interfacial roughness causes PMA to decrease.

However, as seen from figure 3 changes in PMA do not correlate with the changes in the interface roughness. Therefore, the observed decrease in PMA with dose cannot be totally attributed to the increase in the interfacial roughness. The atomic rearrangements associated with the electronic energy loss should also cause the relaxation of internal stresses in the films, which would result in a decrease in the magnetoelastic contribution to the anisotropy. Thus, the observed decrease in PMA with Si dose is a result of an increase in the interfacial roughness and stress relaxation in the bulk of the films. The initial faster decrease in PMA suggests that most of the structural relaxation has taken place up to an irradiation dose of 10^{14} ions cm^{-2} and the subsequent slow decrease in PMA is mainly due to increase in interfacial roughness.

Irradiation with 150 MeV Ag ions causes the interfacial roughness and the thickness of the intermixed region to increase. Both these effects would cause PMA to decrease. It may be noted that an increase in interfacial roughness from 2.5 to 6.5 Å increases ϕ at the most by $\sim 3.8^\circ$. Therefore in the Ag ion irradiated specimen the contribution of increased interfacial roughness to the observed increase in ϕ should also be of the same order. The rest of the change in ϕ (18.5°) must be attributed to increased intermixing at the interfaces. This suggest that the effect of intermixing on PMA is much stronger than that of the interfacial roughness. It may be noted that in an earlier study by Tosello *et al* of the effect of keV energy ion irradiation on PMA of Fe–Tb multilayers the main effect of the irradiation was to increase the width of the interfacial region (as indicated by an increase in the broad hyperfine field component) [25]. This was accompanied by a large increase in the average angle ϕ between the spin direction and the normal to the film plane. This effect is very similar to the effect of Ag ion irradiation in the present case where an increase in the width of the intermixed region is accompanied by a large decrease in PMA.

Richomme *et al* have studied in detail the effect of swift heavy ion irradiation on PMA on Fe–Tb multilayers. The observed effects have been explained in terms of the change in thickness of the intermixed layer as a result of demixing or mixing at the interfaces. However as pointed out in section 1 the observed changes in PMA do not correlate quantitatively with the changes in the thickness of the intermixed layer. Present studies show that other effects such as changes in interfacial roughness or stress relaxation in the bulk of the layers can also cause the angle ϕ to change by a value as large as about 6°. This change is comparable to the total change observed by Richomme *et al* as a result of various irradiations. Therefore in order to understand the effect of swift heavy ion irradiation on PMA one should also take

into account the effect of changes in interfacial roughness and internal stresses in the film.

5. Conclusion

In conclusion, the effect of swift heavy ion irradiation on Fe–Tb multilayers has been studied. In the case of 80 MeV Si ions, although the electronic energy loss is well below the threshold for mixing to occur, irradiation results in several changes in the multilayer, which include (i) creation of disorder in the bulk of the layers, (ii) stress relaxation, (iii) an increase in the interfacial roughness and (iv) segregation of Fe and Tb atoms in the intermixed region. Increase in the interfacial roughness may be associated with the segregation of Fe and Tb atoms. The observed decrease in the PMA with irradiation is a combined effect of (i) a decrease in magnetoelastic anisotropy associated with stress relaxation and (ii) an increase in the interfacial roughness. In agreement with the earlier studies Ag ion irradiation causes intermixing at the interfaces. The effect of intermixing on PMA is found to be much stronger than that of interfacial roughness.

Acknowledgment

The Fe–Tb multilayers for the present studies were kindly provided by Professor W Keune of the University of Duisberg, Germany.

References

[1] Sato N 1986 *J. Appl. Phys.* **59** 2514
[2] Scholz B, Brand R A and Keune W 1992 *J. Magn. Magn. Mater.* **104** 1089
[3] Honda S, Nawate M and Sakamato I 1996 *J. Appl. Phys.* **79** 365
[4] Richomme F, Teillet J, Fnidiki A, Auric P and Houdy Ph 1996 *Phys. Rev.* B **54** 416
[5] Tappart J, Keune W and Brand R A 1996 *J. Appl. Phys.* **80** 4503
[6] Scholz B, Brand R A and Keune W 1994 *Phys. Rev.* B **50** 2537
[7] Shan Z S, Sellmyer D J, Jaswal S S, Wang Y J and Shen J X 1990 *Phys. Rev.* B **42** 10 446
[8] Findiki A, Juraszek J, Teillet J, Richomme F and Lebertois J P 1997 *J. Magn. Magn. Mater.* **165** 405
[9] Cherifi K, Dufour C, Piecuch M, Bruson A, Bauer Ph, Marchal G and Mangin Ph 1991 *J. Magn. Magn. Mater.* **93** 609
[10] Richomme F, Findiki A, Teillet J and Toulemonde M 1996 *Nucl. Instrum. Methods* B **107** 374
[11] Teillet J, Richomme F and Fnidiki A 1997 *Phys. Rev.* B **55** 11 560
[12] Toulemonde M and Dufour C 1992 *Phys. Rev.* B **42** 14 362
[13] Huang T C and Parrish W 1992 *Adv. X-ray Anal.* **35** 137
[14] Parratt L G 1954 *Phys. Rev.* 359
[15] Underwood J H and Barbee T W Jr 1981 *Appl. Opt.* **20** 3027
[16] Sinha S K, Sirota E B, Garoff S and Stanley H B 1988 *Phys. Rev.* B **38** 2297
[17] Brand R A 1987 *Nucl. Instrum. Methods* B **28** 398
[18] Usami K, Kobayashi N and Miyauchi A 1993 *Japan. J. Appl. Phys.* **32** 3312
Stettner J, Schwalowsky L, Seeck O H, Tolan M, Press W, Schwarz C and v Känel H 1996 *Phys. Rev.* B **53** 1398
[19] Itoh N 1990 *Radiat. Eff. Defects Solids* **110** 19
[20] Dunlop A and Leseur D 1992 *Mater. Sci. Forum* **97–99** 553
[21] Barbu A, Dunlop A, Lesuere D and Averbeck R S 1991 *Europhys. Lett.* **15** 37
[22] Dufour C, Bauer Ph, Marchal G, Grilhe J, Jaouen C, Pacaud J and Jousset J C 1993 *Europhys Lett.* **21** 671
[23] Draaisma H J G, den Broeder F J A and de Jonge W J M 1987 *J. Magn. Magn. Mater.* **66** 351
[24] den Broeder F J A, Hoving W and Bloemen P J H 1991 *J. Magn. Magn. Mater.* **93** 562
[25] Tosello C, Gratton L M, Principi G, Gupta A and Gupta R 1996 *Sur. Coating Technol.* **84** 338